THE IMPACT OF THE DROPWINDSONDE DATA FROM DOTSTAR ON THE TRACK PREDICTION OF TYPHOON CONSON (2004)

10A.5

Wei-Peng Huang, Chun-Chieh Wu*, Po-Hsiung Lin, and Kun-Hsuan Chou

Department of Atmospheric Sciences, National Taiwan University, Taipei, Taiwan

1. INTRODUCTION

Tropical cyclones (TC) generally develop in the data-sparse oceanic regions. Therefore, the lack of observations has always been a major problem affecting the accuracy of TC forecasts. In 1982, the Hurricane Research Division (HRD) began to investigate possible improvements on numerical TC track forecasts with the assimilation of dropwindsonde observations made in the data-sparse TC environment. The observation helped the National Centers for Environmental Prediction (NCEP) and the Geophysical Fluid Dynamics Laboratory (GFDL) hurricane model to reduce track forecast errors significantly (Burpee et al. 1996). The follow-up dropwindsonde data obtained from the Gulf Stream-IV aircraft surveillance also show significant impact on the hurricane track prediction (Aberson and Franklin 1999; Aberson 2003).

Considering the potential of dropwindsonde data for improving typhoon forecasts, a research project, Dropsonde Observations for Typhoon Surveillance near the Taiwan Region (DOTSTAR; Wu et al. 2005) was developed to conduct surveillance missions for typhoons in the western North Pacific from 2003. Up to now, 15 typhoons have been observed in 19 missions, with a total of 313 dropwindsondes released.

In this paper, we focus on the evaluation of the impact of the dropwindsondes on the track of Typhoon Conson (2004).

2. METHODOLOGY AND EXPERIMENT DESIGN

The three-dimensional variational (3D-VAR) data assimilation system for use with the fifth-generation Pennsylvania State University-NCAR Mesoscale Model (MM5) (Barker et al. 2003; 2004) is utilized to assimilate the dropwindsonde data. The background field is from the NCEP GFS (Global Forecasting System) global analysis (1°×1°) without assimilating dropwindsonde data. The cost function of MM5 3D-VAR is defined as:

$$J(x) = J^b + J^o$$
$$= \frac{1}{2}(x - x^b)^T B^{-1}(x - x^b) + \frac{1}{2}(Hx - y^o)^T O^{-1}(Hx - y^o),$$

where J^b is the background term, J^o is the observation term, x is the analysis variable vector, x^b is the background variable vector, y is the observation vector, and H is the nonlinear operator to transform the analysis variable vector to the observation vector. The 3D-VAR solution x is obtained for the analysis that minimizes the total cost function. Therefore the model space vector is the best simultaneous fit between the background vector and the observation vector.

After assimilating the dropwindsonde data by MM5 3D-VAR, MM5 is run for 72 h. And the experiment is referred to as 3DVAR. To evaluate the impact of the dropwindsonde data, another experiment, which is referred to as CTL, is performed. The GFS analysis without assimilating the dropwindsonde data is used as the model's initial data in CTL.

More experiments are conducted to examine the impact from different subsets of the dropwindsonde data, the data assimilation schemes, the presence of Taiwan terrain and the bogusing scheme to the typhoon track simulation. All experiments are listed in Table 1.

* *Corresponding author address:*
Chun-Chieh Wu, Department of Atmospheric Sciences, National Taiwan University, No. 1, Sec. 4, Roosevelt Rd., Taipei 106, Taiwan;
E-mail: cwu@typhoon.as.ntu.edu.tw

Table 1. The experiment design

Exp.	Dropsonde data	DA scheme	Others
CTL	None	X	
3DVAR	All	3DVAR	
3DVAR-N10	Northern 10 drops	3DVAR	
3DVAR-S6	Southern 6 drops	3DVAR	
3DVAR-1000850	1000-850 hPa	3DVAR	
3DVAR-700400	700-400 hPa	3DVAR	
3DVAR-300200	300-200 hPa	3DVAR	
3DVAR-850300	850-300 hPa	3DVAR	
CRSSMN	All	Cressman	
CTL-nTW	None	X	No Taiwan
3DVAR-nTW	All	3DVAR	No Taiwan
CTL-BG	None	X	bogused
3DVAR-BG	All	3DVAR	bogused

3. RESULTS

a. Comparison of CTL and 3DVAR

(1) Differences of initial fields and tracks

The 925-200-hPa deep layer mean (DLM) wind differences of 3DVAR and CTL show that the maximum increment is up to 7 m s^{-1} in the southern area where the dropwindsondes were released (Fig. 1.). Therefore, the impact of the dropwindsondes on the initial field is significant in this case.

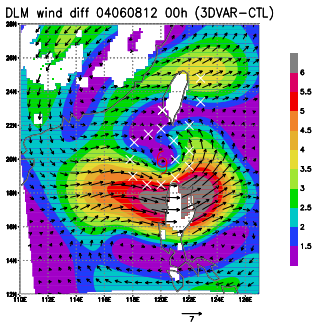

Figure 1. The differences of DLM winds between 3DVAR and CTL at initial time (Arrows indicate wind vectors and shading indicates wind speeds). The locations where the dropwindsonde are deployed are indicated with "x"

The track simulation of CTL and 3DVAR is shown in Fig. 2. The tracks of the two experiments start to divert from each other after 6 h. The typhoon in CTL moves toward the west, while that of 3DVAR keeps moving northeastward, which is in better agreement with the best tracks. Figure 3 indicates that the track errors of 3DVAR are much smaller than that of CTL during the whole simulation period, and the averaged improvement of 3DVAR over CTL is 56%.

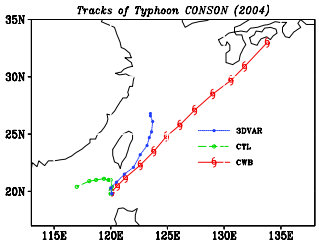

Figure 2. The best track (CWB) and the simulated tracks of 3DVAR and CTL.

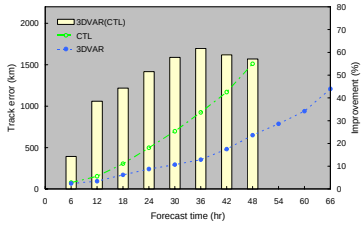

Figure 3. The simulated track errors of 3DVAR and CTL. Dash lines indicate errors (unit: km) and the bars indicate the improvement of 3DVAR over CTL (unit: %).

(2) Potential vorticity inversion diagnosis

To figure out which factor causes the different simulated tracks between the two experiments, piecewise potential vorticity (PV) inversion (Wu et al. 2003; 2004) is performed for the 6-h forecast. The fields of CTL are regarded as the basic fields and those of 3DVAR as the total fields. In this way, the perturbation fields are the differences between the two runs, and the perturbations are divided into several parts to investigate how the flow attributed to each PV anomaly affects the motion of the typhoon. The two equations to be solved are

$$q=\frac{gk\pi}{p}\left[(f+\nabla^2\Psi)\frac{\partial^2\Phi}{\partial\pi^2}-\frac{1}{a^2\cos^2\phi}\frac{\partial^2\Psi}{\partial\lambda\partial\pi}\frac{\partial^2\Phi}{\partial\lambda\partial\pi}-\frac{1}{a^2}\frac{\partial^2\Psi}{\partial\phi\partial\pi}\frac{\partial^2\Phi}{\partial\phi\partial\pi}\right] ,$$

and $$\nabla^2\hat{\Phi}=\nabla\cdot(f_0\nabla\Psi)+\frac{2}{a^4\cos^2\phi}\frac{\partial(\partial\Psi/\partial\lambda,\partial\Psi/\partial\phi)}{\partial(\lambda,\phi)} ,$$

where q represents potential vorticity, Φ represents geopotential height, Ψ represents streamfunction, a is the earth's radius, f is the Coriolis parameter, $\kappa=R_d/C_p$, λ is latitude, and φ is longitude. Given the distribution of q, the lateral boundary Φ and Ψ, and the θ on the upper and lower boundary, the distribution of Φ and Ψ can be solved.

As shown in Fig. 4, different pieces of the PV perturbations are numbered. The contribution of each PV anomaly to Conson's DLM steering flow at 6 h is shown in Fig. 5. The results indicate that the no. 1 PV anomaly is the key factor in steering the simulated typhoon of 3DVAR northeastward relative to that of CTL. On the other hand, the other 4 PV anomalies are less significant to the steering flow of the typhoon.

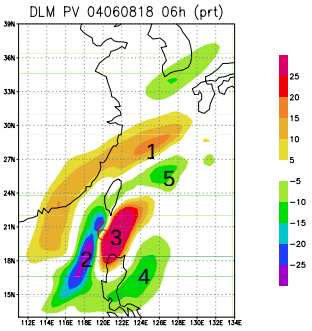

Figure 4. The DLM PV perturbations at 6h. (unit: PVU*10^2)

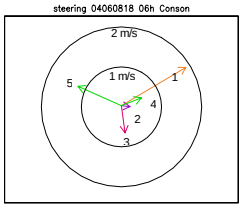

Figure 5. The balanced flow averaged over inner 3^o around the TC center associated with corresponding number of PV anomaly at 6-h

b. Impact study

(1) Horizontal distribution of dropwindsonde data

To evaluate the impact of the horizontal distribution of the dropwindsonde data, the 16 drops gathered in the mission are divided into two subsets: the 10 dropwindsondes to the north (referred to as 3DVAR-N10) and the 6 dropwindsondes to the south (referred to as 3DVAR-S6) (see Fig. 6). The corresponding model tracks (Fig. 7) show that both experiments make Conson move northeastward along the east coast of Taiwan. It is also found in Fig. 8 that 3DVAR-S6 in general has a smaller track error as compared to 3DVAR-N10. This is consistent with the finding in Fig. 1 that DLM wind increments due to the dropwindsonde assimilation are much larger to the south (3DVAR-S6) than to the north (3DVAR-N10).

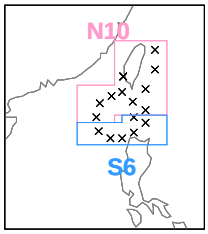

Figure 6. The dropwindsonde distribution of 3DVAR-N10 and 3DVAR-S6.

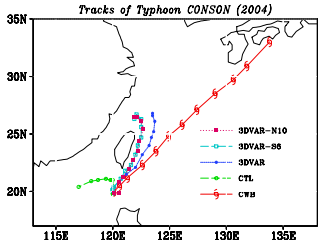

Figure 7. The best track (CWB) and the simulated tracks of CTL, 3DVAR, 3DVAR-S6 and 3DVAR-N10.

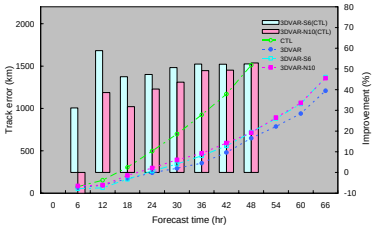

Figure 8. The model track errors of 3DVAR-N10, 3DVAR-S6, 3DVAR and CTL. Dash lines indicate errors (unit: km) and bars indicate the improvement of each experiment over CTL (unit: %).

(2) Vertical distribution of dropwindsonde data

The impact from the vertical distribution of the dropwindsonde data is investigated. Four different experiments are performed to assimilate dropwindsonde data from different levels, i.e., the low level (1000-850 hPa, referred to as 3DVAR-1000850), the middle level (700-400 hPa, referred to as 3DVAR-700400), the high level (300-200 hPa, referred to as 3DVAR-300200), and the deep level (850-300 hPa, referred to as 3DVAR-850300). The track simulation (Fig. 9) shows that except for 3DVAR-300200, the simulated typhoons in the other three experiments move northeastward, in better agreement with the best track. The simulated track of 3DVAR-300200 is similar to that of CTL, which turns Conson to the west over South China Sea. Since Conson is a rather weak system, the steering level is not likely to reach the upper troposphere. This explains the lack of track improvement from the dropwindsondes in the upper level as in 3DVAR-300200. Among all the experiments in this section, the 3DVAR-850300 provides the most track forecast improvement (Fig. 10) which is very much consistent with our intuition that the assimilation of the entire DLM wind should best improve the track forecast.

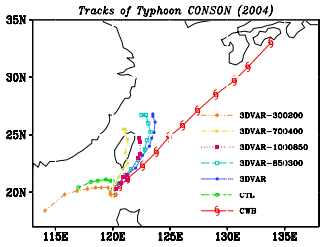

Figure 9. The best track (CWB) and the simulated tracks of CTL and all experiments in section (2).

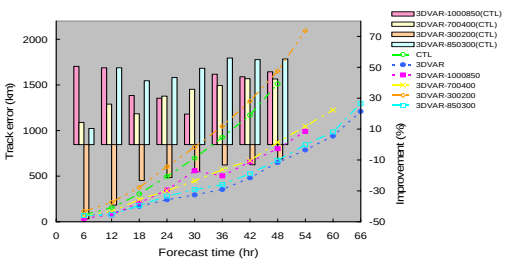

Figure 10. The simulated track errors of 3DVAR-850300, 3DVAR-300200, 3DVAR-700400, 3DVAR-1000850, 3DVAR and CTL. Dash lines indicate errors (unit: km) and bars indicate the improvement of each experiment over CTL (unit: %)

(3) Different data assimilation schemes

Not only the observation itself but also the data assimilation schemes play an important role in affecting the model performance. To investigate the effect of the different assimilation schemes on the impact of the dropwindsonde data on the model track prediction, the Cressman scheme (Cressman 1959) is conducted (denoted as CRSSMN). The DLM wind differences between 3DVAR and CTL (between CRSSMN and CTL), are shown in Fig. 11a (Fig. 11b). The distribution of the DLM wind increment in Figs. 11a and 11b is very different. The simulated track in CRSSMN (Fig. 12) moves more northward than that in CTL, yet still does not catch the correct northeastward movement. The track errors of CRSSMN and 3DVAR are shown in Fig. 13. The averaged improvement of CRSSMN is 13%, which is much lower than that associated with 3DVAR.

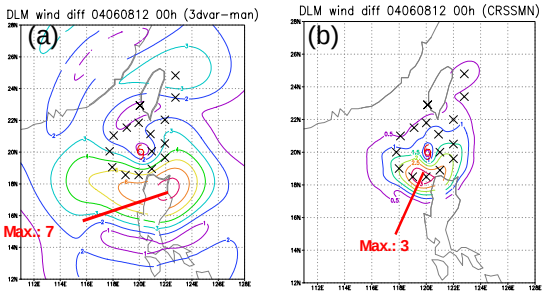

Figure 11 The DLM wind differences (a) between 3DVAR and CTL; (b) between CRSSMN and CTL.

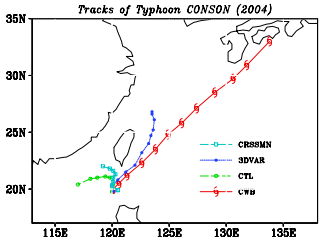

Figure 12. The best track (CWB) and the simulated tracks of CTL, 3DVAR and CRSSMN.

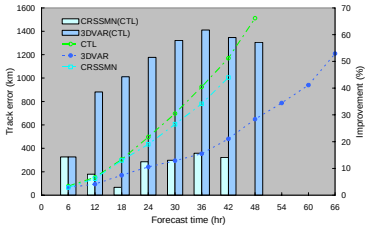

Figure 13. The simulated track errors of CRSSMN, 3DVAR and CTL. Dash lines indicate errors (unit: km) and bars indicate the improvement of CRSSMN and 3DVAR over CTL (unit: %).

(4) The impact from Taiwan terrain

Since Conson occurs close to the southern tip of Taiwan, it is interesting to know whether the presence of the Taiwan terrain may have played a role in affecting the track of Conson. Therefore, two extra experiments, denoted as CTL-nTW and 3DVAR-nTW, are performed in both CTL and 3DVAR, but without the Taiwan terrain. The similar model tracks in Fig. 14 suggest that the Taiwan terrain is not a crucial factor in affecting the track simulation. Simulations in both 3DVAR and 3DVAR-nTW have much smaller track errors than those in both CTL and CTL-nTW, indicating that the assimilation of the dropwindsonde data plays the key role in improving the track of Conson, whether the Taiwan terrain is present or not.

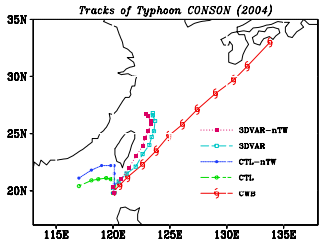

Figure 14. The best track (CWB) and the simulated tracks of CTL, CTL-nTW, 3DVAR and 3DVAR-nTW.

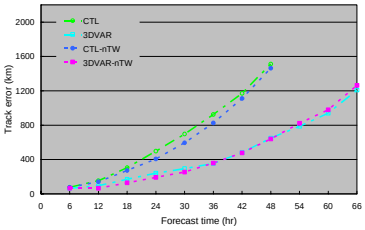

Figure 15. The simulated track errors of 3DVAR-nTW, CTL-nTW, 3DVAR and CTL.

(5) Impact from the bogused storm vortex

The initial minimum central sea level pressure of the typhoon vortex in CTL is 1005 hPa, which is much weaker compared to the estimated intensity of 970 hPa from the best-track analysis of CWB. To have a better representation of the initial vortex strength, a bogused procedure (Davis and Low-Nam 2001) is added during the model initialization in the experiments of CTL and 3DVAR (denoted as CTL-BG and 3DVAR-BG). Although the initial vortices of CTL-BG and 3DVAR-BG decrease quickly when the simulation begins, both simulated tracks are in better agreement with the best track (Fig. 16). The errors and improvement of the CTL-BG and 3DVAR-BG (Fig. 17) indicate that the averaged 48-h improvement of 3DVAR-BG over CTL is 70%, while the improvement of 3DVAR over CTL is 56% only. The above result indicates that both a good representation of the initial bogused TC vortex and the assimilation of dropwindsonde data can lead to a very good track improvement.

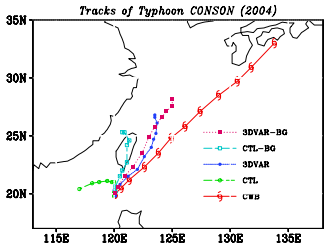

Figure 16. The best track (CWB) and the simulation tracks of CTL, 3DVAR, CTL-BG and 3DVAR-BG.

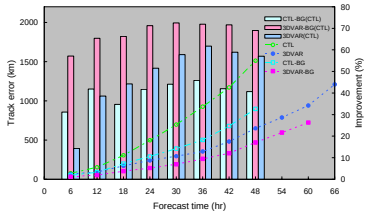

Figure 17. The simulated track errors of 3DVAR-BG, CTL-BG, 3DVAR and CTL. Dash lines indicate errors (unit: km) and bars indicate the improvement of each experiment over CTL (unit: %).

4. SUMMARY

In this work, the MM5 3D-VAR system is utilized to assimilate the dropwindsonde data from DOTSTAR and to investigate the impact of the data on the track forecast of Typhoon Conson (2004). It is shown that the impact of the dropwindsonde on the initial field (as depicted by the DLM wind differences) and the subsequent track forecast is significant, regardless whether the Taiwan terrain is present or not. The potential vorticity diagnosis is performed in the analyses to investigate the key factor in affecting the motion of the typhoon.

The study for examining the impact from different subsets of the dropwindsonde data shows that the dropwindsonde data in the low and middle troposphere is more effective in improving the track forecast of the weak Conson than those in the upper troposphere. It is also demonstrated that both a good representation of the initial bogused TC vortex and the assimilation of dropwindsonde data can lead to better track simulation.

In addition, the results of the impact study show that not only the observation itself but also the data assimilation schemes play an important role in affecting the model performance. Further studies will also be conducted to assess the impact from other data assimilation schemes (such as the four-dimensional variational data assimilation; Wu et al. 2006).

References

Aberson, S. D., and J. L. Franklin, 1999: Impact on hurricane track and intensity forecasts of GPS dropwindsonde observations from the first-season flights of the NOAA gulf stream-IV Jet Aircraft. *Bull. Amer. Meteor. Soc.*, **80**, 421-427.

_____, 2003: Targeted observations to improve operational tropical cyclone track forecast guidance. *Mon. Wea. Rev.*, **131**, 1613-1628.

Barker, D. M., W. Huang, Y.-R. Guo, and A. J. Bourgeois, 2003: A three-dimensional variational (3DVAR) data assimilation system for use with MM5. MMM Division, NCAR, P.O. Box 3000, Boulder, CO, 80307-3000, USA.

_____, W. Huang, Y.-R. Guo, A. J. Bourgeois and Q. N. Xiao, 2004: A three-dimensional variational data assimilation system for MM5: Implementation and initial results. *Mon. Wea. Rev.*, **132**, 897–914.

Burpee, R. W., J. L. Franklin, S. J. Lord, R. E. Tuleya, and S. D. Aberson, 1996: The impact of Omegadropwindsondes on operational hurricane track forecast models. *Bull. Amer. Meteor. Soc.*, **77**, 925-933.

Cressman, G. P., 1959: An operational objective analysis system. *Mon. Wea. Rev.*, **87**, 367–374.

Davis, C. A., and S. Low-Nam, 2001: The NCAR-AFWA tropical cyclone bogussing scheme. A report prepared for the Air Force Weather Agency (AFWA). National Center for Atmospheric Research, Boulder, Co, USA.

Wu, C.-C., T.-S. Huang, W.-P. Huang, and K.-H. Chou. 2003: A new look at the binary interaction: Potential vorticity diagnosis of the unusual southward movement of tropical storm Bopha (2000) and its interaction with Supertyphoon Saomai (2000). *Mon. Wea. Rev*, **131**, 1289–1300.

_____, T.-S. Huang, and K.-H. Chou, 2004: Potential vorticity diagnosis of the key factors affecting the motion of Typhoon Sinlaku (2002). *Mon. Wea. Rev.,* **132**, 2084–2093.

_____, P.-H. Lin, S. Aberson, T.-C. Yeh, W.-P. Huang, K.-H. Chou, J.-S. Hong, G.-C. Lu, C.-T. Fong, K.-C. Hsu, I-I Lin, P.-L. Lin, and C.-H. Liu, 2005: Dropwindsonde Observations for Typhoon Surveillance near the Taiwan Region (DOTSTAR): An overview. *Bull. Amer. Meteor. Soc.*, **86**, 787-790.

_____, K.-H. Chou, Y. Wang and Y.-H. Kuo, 2006: Tropical cyclone initialization and prediction based on four-dimensional variational data assimilation. *J. Atmos. Sci.* (in press)